Study of the TiO_2−H_2O−B_2O_3 Ternary System at 7.7 GPa and High Temperatures

Rommulo V. Conceição,[†] Sérgio R. S. Soares,[†] Naira M. Balzaretti,[†] Altair S. Pereira,[†,||] Tania M. H. Costa,[†,‡] Márcia R. Gallas,*[,†] and João A. H. da Jornada[†,§]

Instituto de Física, UFRGS, Caixa Postal 15051, 91501-970 Porto Alegre (RS), Brazil, Instituto de Química, UFRGS, Caixa Postal 15003, 91501-970 Porto Alegre (RS), Brazil, INMETRO, Av. Nossa Senhora das Graças 50, 25250-020 Xerem, (RJ), Brazil, and Escola de Engenharia, UFRGS, Av. Osvaldo Aranha 99, 90035-190. Porto Alegre, (RS), Brazil

Received April 12, 2001. Revised Manuscript Received September 26, 2001

The TiO_2−H_2O−B_2O_3 ternary system was studied at high pressure (7.7 GPa) and high temperatures, and a phase diagram is proposed. Depending on the initial stoichiometric conditions, Raman spectral analysis identified rutile, TiO_2-II, H_3BO_3, HBO_2, and B_2O_3 as the crystalline stable phases, and an amorphous phase constituted by B, Ti, and O. The eutectic point of this system was identified to be at around 400 °C. Two piercing points were located at around 600 and 1100 °C, identified by the stabilization of HBO_2 rather than H_3BO_3, and B_2O_3 rather than HBO_2, respectively. This study shows that TiB_2 sintering at high pressure can be compromised by the presence of oxide-bearing phases that decrease the eutectic point of the system. This phenomenon can produce a liquid that works as a medium for transporting material, producing grain growth, which compromises the boride properties.

Introduction

Borides have been studied extensively due to their potential applications in electrodes, cutting tools, armor materials, and as reinforcing phase in metal-matrix composites. They have exceptional thermal stability, hardness, and mechanical properties under practical applications.[1] However, the presence of oxygen-bearing phases such as boron oxide (B_2O_3), boric acid (H_3BO_3), and metaboric acid (HBO_2) at the sintering process strongly influences the tribological properties of the borides. Several studies have shown that the presence of these phases causes the anomalous increasing of the boride grain, compromising the density and hardness of the ceramic.[2] The plausible mechanism responsible for such effect is not completely understood. Therefore, the study of the behavior of boron-, oxygen-bearing phases at the sintering conditions is very important.

Until recently, the majority of the experimental studies on the pressure−temperature stability relation of oxygen-, boron-bearing minerals, under hydrous or anhydrous conditions, were developed especially with a geological interest through phase diagram studies. Kracek[3] developed the first studies in a binary system near ambient pressure, in which the end members were B_2O_3 and H_2O. He observed that at this pressure the melting point of B_2O_3 is around 450 °C, and there is full fluid miscibility between the components H_2O and B_2O_3. In this system, the solid binary phases are H_3BO_3 (sassolite) and HBO_2 (metaborite) that can occur as cubic (HBO_2-I), monoclinic (HBO_2-II), or orthorhombic (HBO_2-III). At 1 atm, cubic, monoclinic, and orthorhombic metaboric acid melt at 236, 200, and 176 °C, respectively. H_3BO_3 melts incongruently to cubic metaboric acid at 169 °C at 1 atm. Pereira et al.[4] observed that when submitted to high pressure, H_3BO_3 breaks down to cubic metaboric acid and water. The addition of other materials, such as SiO_2 and Al_2O_3 to the B−O−H-system was made by Rockett and Foster,[5] Pichavant,[6] Gielisse and Foster.[7] At 1 atm, B_2O_3 is completely miscible in the system B_2O_3−SiO_2 and B_2O_3−Al_2O_3 above the liquidus. However, a tendency to B-rich-liquid versus B-poor-liquid immiscibility can be observed. It occurs mainly by the presence of metastable liquid−liquid immiscibility reported in the B_2O_3−SiO_2[6] and B_2O_3−M_2O (M = alkali metal)[8] binary systems, and in the SiO_2−B_2O_3−(Na_2O/K_2O)[9,10] ternary system. Stable liquid−liquid immiscibility is known to occur in the ternary systems SiO_2−B_2O_3−MO (M = Ca, Ba).[11,12] In all these systems, except the SiO_2−B_2O_3−H_2O, there is

* Corresponding author. Telephone: (55)(51)33166542. Fax: (55)(51)-33167286. E-mail: marcia@if.ufrgs.br.
[†] Instituto de Física, UFRGS.
[‡] Instituto de Química, UFRGS.
[§] INMETRO.
[||] Escola de Engenharia, UFRGS.

(1) Tennery, V. J.; Finch, C. B.; Yust, C. S.; Clark, G. W. *Science of Hard Material*; Plenum: New York, 1983.
(2) Finch, C. B.; Becher, P. F.; Angelini, P.; Baik, S.; Bamberger, C. E.; Brynestad, *J. Adv. Ceram. Mater.* **1986**, *1*, 50.
(3) Kracek, F. C.; Morey, G. W.; Merwin, H. E. *Am. J. Sci.* **1938**, *35-A*, 145.
(4) Pereira, A. S.; Perotonni, C. A.; Jornada, J. A. H., manuscript to be published.
(5) Rockett, T. J.; Foster, W. R. *J. Am. Ceram. Soc.* **1965**, *48*, 75.
(6) Pichavant, M. *Bull. Miner.* **1978**, *106*, 201.
(7) Gielisse, P. J.; Foster, W. R. *Nature* **1962**, *197*, 69−70.
(8) Shaw, R. R.; Uhlmann, D. R. *J. Am. Ceram. Soc.* **1968**, *51*, 377.
(9) Haller, W.; Blackburn, D. H.; Wagstaff, F. E.; Charles, R. J. *J. Am. Ceram. Soc.* **1970**, *53*, 34.
(10) Taylor, P.; Owen, D. G. *J. Am. Ceram. Soc.* **1981**, *64*, C158.
(11) Morey, G. W.; Ingerson, E. *Am. Mineral.* **1937**, *22*, 37−47.
(12) Vogel, W. *J. Non-Cryst. Solids* **1977**, *25*, 170.

10.1021/cm0103242 CCC: $22.00
Published on Web 12/08/2001

always a hydrous and/or an anhydrous ternary phase. Among them, anhydrous Al−O−B-bearing phases have shown many applications in material science.

Contrasting to this background, few studies have been made in the B−Ti−O system. Finch et al.[2] suggest that oxygen content is one of the main limitations to obtain high densification during hot pressing sintering of TiB_2. For powders of TiB_2 containing more than 1 wt % oxygen, only 75 to 90% of the theoretical density is reached after the sintering process by vacuum hot-pressing (1400 to 1700 °C). Baik and Becher[13] made several densification studies in this ceramic material. They noticed that under hot-pressing densification process, the presence of oxygen, as the B_2O_3 phase, makes the TiB_2 grain to grow fast by an evaporation−condensation kinetics process, limiting the maximum attainable densification. They suggest that samples with 1.7 wt % oxygen can reach only 85% of the theoretical density, while samples with 0.7 wt % reach around 95%. Under pressureless sintering, they suggest that B_2O_3 is evaporated due to its low vapor pressure, and oxygen is only present as TiO_2. In this case, the samples can reach the maximum of the theoretical density; however, the fast grain growth still occurs and is caused by a surface diffusivity process. Pavlikov et al.[14] worked at 1 atm in the $B_2O_3-TiO_2$ system and identified an eutectic point between 400 and 450 °C. They suggested a possible liquid−liquid immiscibility close to the liquidus.

As a consequence of the high difficulty to obtain well-sintered boride compacts, alternative sintering techniques have been proposed in the literature.[2,4] Among these techniques, high-pressure sintering can be a very interesting option. This technique promotes an improvement of the powder compaction and allows the use of lower temperatures and shorter sintering times. This possibility is very important to control grain growth and its deleterious effects, mainly over the mechanical properties of the sintered body.

In this way, the study of the phase diagram under high pressure and high temperature of the phases usually observed in the boride powder is of great interest.

As far as we know, there are no published studies of the system $TiO_2-H_2O-B_2O_3$ under high pressure and high temperature. We believe the stable phases present in this system play a decisive role in the sintering mechanism of TiB_2. In this work, we investigate this system at 7.7 GPa to study the possible stabilization of a ternary phase and the miscibility of those components and liquids, and we propose a schematic phase diagram for this system.

Experimental Methodology

Starting Material. The starting materials used were a stoichiometric mixture of crystalline H_3BO_3 + crystalline HBO_2(II) + vitreous B_2O_3 + H_2O and TiO_2 (anatase + rutile). The Raman spectra of these phases are shown in Figure 1. Crystalline HBO_2 (II) was obtained by partial dehydration of crystalline H_3BO_3 (P. A.) at 1 atm and 120 °C for one week. Vitreous B_2O_3 was obtained by total dehydration of H_3BO_3 at 1000 °C for 3 days. After obtaining these two components, each one was mixed and finely ground with TiO_2 in a stoichiometric proportion. HBO_2 + TiO_2 was heated for 2 days at 1 atm and 120 °C, and vitreous B_2O_3 + TiO_2 was heated for 1 day at 1 atm and 1000° C. Mixtures with H_3BO_3 and TiO_2 were also prepared. All mixtures were kept in the oven at 100 °C before the experiment. At this temperature, H_3BO_3 does not degrade, and the addition of water in the mixtures is avoided. As HBO_2 and B_2O_3 easily absorb water and transform to H_3BO_3, Raman spectroscopy was used to estimate the phases present in the mixtures before the experiments. However, even taking maximum care, B_2O_3 invariably reacts with water, introducing uncertainties in the B_2O_3/H_2O ratios. The compositions of all starting materials are listed in Table 1 in terms of the molar fraction of end members: B_2O_3, TiO_2, and H_2O. To make the composition #1 of the starting material, in which an H_2O-oversaturated condition is necessary, additional water was stoichiometrically added by a microsyringe.

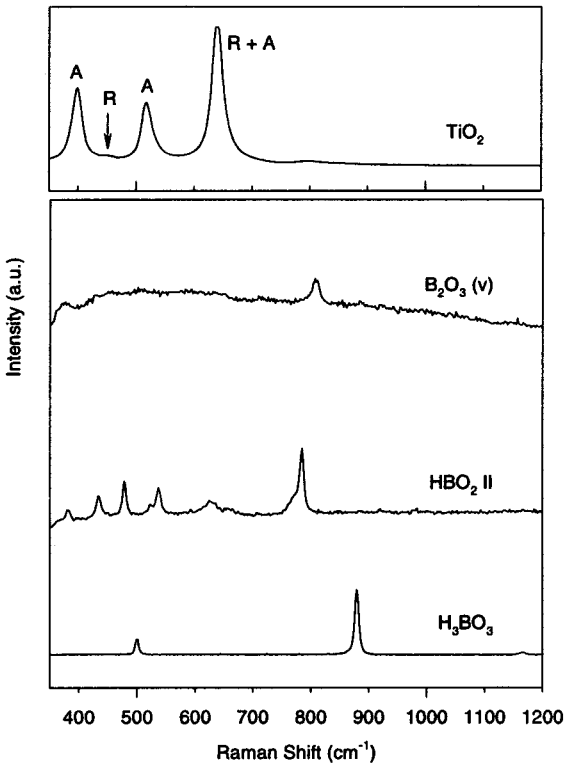

Figure 1. Raman spectra for the starting materials. The peaks marked with A correspond to the anatase phase, and those marked with R correspond to the rutile phase.

Table 1. Compositions of the Starting Materials

starting material	B_2O_3 (mol %)	TiO_2 (mol %)	H_2O (mol %)
#1	15.00	15.00	70.00
#2	20.00	20.00	60.00
#3	33.30	33.30	33.30
#4	45.00	45.00	10.00

High-Pressure Processing. All the experiments were performed in a high-pressure toroidal-type chamber, and a detailed description of this high-pressure method is given elsewhere.[15,16] The temperature was controlled to ± 3 °C and was measured with a Chromel-Alumel type K thermocouple encapsulated in an Al_2O_3 sleeve. The pressure cells consisted of a graphite heater (height of 9.2 mm, diameter of 7.0 mm, and wall thickness of 1.5 mm), and two small disks of fired pyrophyllite (diameter of 4.0 mm, and height of 1.5 mm). A capsule with the sample was placed between these two disks. All experiments up to 800 °C were conducted in a hBN capsule (3.0 mm internal diameter). For experiments at higher tem-

(13) Baik, S.; Becher, P. F. *J. Am. Ceram. Soc.* **1987**, *70*, 527.
(14) Pavlikov, V. N.; Yurchenko, V. A.; Tresvyatskii, S. G. Russ. *J. Inorg. Chem.* **1976**, *21*, 126.
(15) Sherman, W. F.; Stadtmuller, A. A. *Experimental Techniques in High-Pressure Research*; John Wiley & Sons Ltd.: London, 1987.
(16) Khvostantsev, L. G. *High Temp. − High Pressures* **1984**, *16*, 165.

Table 2. Summary of the Experimental Results

sample	starting material	temp (°C)	time (min)	phases observed
BTO-1	#1	RT	90	R[a] + A[b] + H_3BO_3
BTO-2	#1	250	90	R + A + H_3BO_3
BTO-3	#1	350	90	TiO_2-II + H_3BO_3
BTO-4	#1	450	90	TiO_2-II + H_3BO_3 + Gl[c]
BTO-5	#1	600	60	TiO_2-II + H_3BO_3 + Gl
BTO-6	#1	750	60	TiO_2-II + HBO_2 + Gl
BTO-7	#1	850	60	R + HBO_2 + Gl
BTO-8	#1	900	60	R + Gl
BTO-12	#2	600	90	TiO_2-II + HBO_2 + Gl
BTO-13	#2	750	60	TiO_2-II + HBO_2 + Gl
BTO-15	#2	850	60	R + Gl
BTO-19	#3	600	90	TiO_2-II + HBO_2 + Gl
BTO-20	#3	750	60	TiO_2-II + HBO_2 + Gl
BTO-21	#3	850	60	R + HBO_2 + Gl
BTO-22	#3	950	60	R + Gl
BTO-23	#4	800	100	R + HBO_2 + Gl
BTO-24	#4	900	100	R + HBO_2 + Gl
BTO-25	#4	1000	100	R + B_2O_3 (?) + Gl
BTO-26	#4	1200	100	R + Gl

[a] R, titanium dioxide, rutile form; [b] A, titanium dioxide, anatase form; [c] Gl, glass phase.

peratures, graphite capsules (2.0 mm internal diameter) were used, placed inside a hBN ring of 3.0 mm internal diameter. The hBN acts as a nearly hydrostatic pressure-transmitting medium and, at lower temperature experiments (up to 800 °C), it behaves as an inert material.

In a typical experiment, pressure was initially applied to the sample cell to a particular value at room temperature. After pressure stabilization, the sample was heated to the final temperature. Quenching was processed by turning off the heating power, and, after 5 to 10 min, the pressure was released. The pressure calibration was performed by the "fixed points" technique, using Bi and Yb, which allowed the calibration of the pressure in the following three fixed points: Bi with phase transitions at 2.5 and 7.7 GPa, and Yb with a phase transition at 4.0 GPa.[15] The pressure is considered accurate to ± 0.5 GPa.

The processing time varied from 4 to 100 min, chosen by the observation of the stabilization of boride phases in time-experiment tests.

Analytical Techniques. All starting material powders and the processed samples were analyzed by micro-Raman spectroscopy and X-ray diffraction analysis. The processed samples, after polishing, were inspected also by reflected light microscopy, SEM (scanning electron microscopy) and EDS (energy dispersive spectroscopy), which helped the phase identification.

X-ray diffraction patterns were obtained with a Siemens diffractometer D500. The micro-Raman spectra of each phase were excited with the 632.8 nm line of a 10 mW HeNe laser, focused in about 2 μm. The laser power was low enough to avoid any damage to the sample. The scattered light was filtered by a super Notch Plus filter and collected by a nitrogen cooled CCD (charged coupled device) detector coupled to a single-monochromator during an acquisition time of 20 to 80 s. The wavelength calibration was made through the spectrum of a Ne spectroscopic lamp, ensuring a wavenumber accuracy better than 1 cm^{-1}. The Raman shift range considered was from 350 to 2250 cm^{-1}. The spectra were collected from different microscopic regions of the same processed sample, after polishing. The distinct regions were identified by optical inspection in the microscope used to record Raman data.

SEM and EDS analysis were obtained using a JEOL, JFM 5800 scanning electron microscope, with an accelerating voltage of 20 kV, and specimen current of 20 nA.

Experimental Results

The experimental results are summarized in Table 2. All the phases were identified by X-ray diffraction and confirmed by micro-Raman spectroscopy.

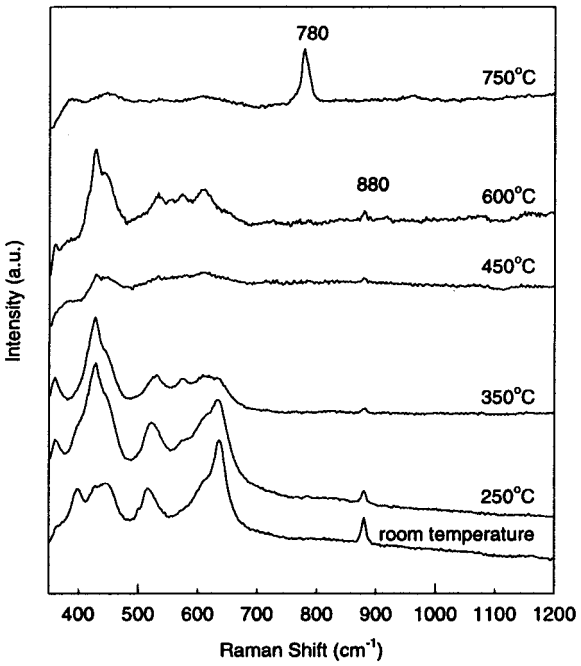

Figure 2. Raman spectra for composition #1 at 7.7 GPa and different temperatures.

The composition #1 corresponds to H_3BO_3 + TiO_2 (1:1), in which 10 mol % of water was added. Raman spectrum of this sample, after the experiment at 7.7 GPa and at room temperature, is displayed in Figure 2, and indicates the presence of boric acid, anatase, and rutile. H_3BO_3 is characterized by the peak at 880 cm^{-1}, that corresponds to the υ_{13} BO_3 breathing mode.[17,18] In the starting material, anatase is characterized by sharp peaks at 393, 515, and 631 cm^{-1}, while rutile is characterized by peaks at 447 and 612 cm^{-1}. However, after processing at room temperature, 7.7 GPa, for 40 min, anatase peaks became broader. The rutile peak at 447 cm^{-1} became broader, and the peak at 612 cm^{-1} shifted to 609 cm^{-1}. Similar results are reported by Mammone et al.,[19] who suggest that the band at 447 cm^{-1} is actually an envelope containing bands from TiO_2-II, a high-pressure polymorph of TiO_2 with the α-PbO_2 structure.[19−21] The Raman spectra remained practically the same for processing at temperatures up to 350 °C, except for the appearance of a sharp peak at 362 cm^{-1}. From this temperature up to 800 °C, TiO_2-II is the stable TiO_2 phase, and it is characterized[18−21] by the Raman peaks at 356, 426, 442, 531, 572, 608, and 820 cm^{-1}. The peak at 880 cm^{-1}, characteristic of the H_3BO_3, decreases up to 600 °C, and at higher temperatures, it is replaced by a sharp peak around 780 cm^{-1}, characteristic of the HBO_2-II.[22,23] This peak remains up to temperatures around 800 °C, when it finally disappears. Experiments conducted above 800 °C, showed

(17) Durig, J. R.; Green, W. H.; Marston, A. L. *J. Mol. Struct.* **1968**, *2*, 19.
(18) Jean, J. H. *J. Appl. Phys.* **1996**, *35*, L429.
(19) Mammone, J. F.; Sharma, S. K.; Nicol, M. *Solid State Commun.* **1980**, *34*, 799−802.
(20) Mammone, J. F.; Nicol, M.; Sharma, S. K. *J. Phys. Chem., Solids* **1981**, *42*, 379.
(21) Bendeliani, N. A.; Popova, S. V.; Vereschagin, L. F. *Geochem. Int.* **1966**, *3*, 387.
(22) Maya, L. *Inorg. Chem.* **1976**, *15*, 2179.
(23) Bertoluzza, A.; Monti, P.; Battaglia, M. A.; Bonora, S. *J. Mol. Struct.* **1980**, *64*, 123.

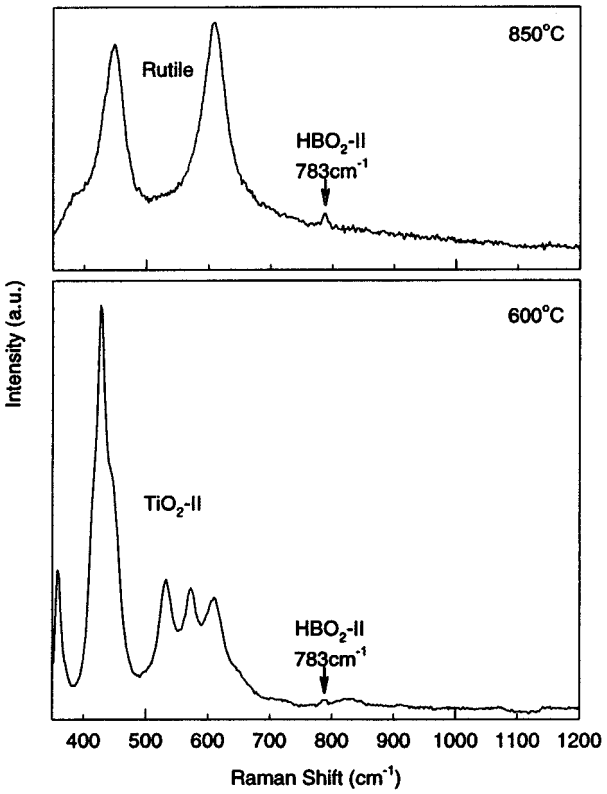

Figure 3. Raman spectra for composition #3 at 7.7 GPa and different temperatures.

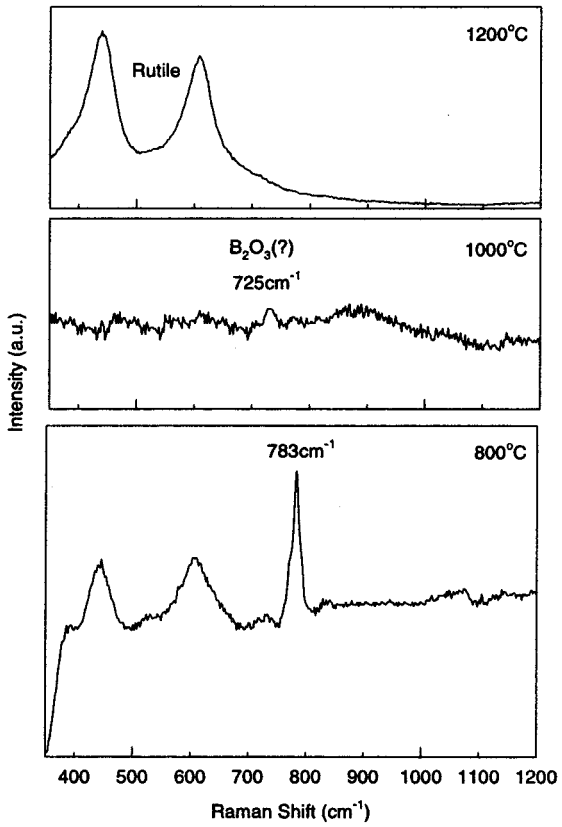

Figure 4. Raman spectra for composition #4 at 7.7 GPa and different temperatures.

that TiO_2-II is replaced by rutile, that is present up to very high temperatures (around 1600 °C). Moreover, above 400 °C, Raman analysis indicated the presence of a very fluorescent material, not observed at lower temperatures. The amount of this material increases at higher temperatures. X-ray diffraction for these samples did not show any other phases besides the ones already identified by micro-Raman analyses, which indicates that this phase could be amorphous. Besides, the texture observed by light optical microscopy and SEM show crystalline grains involved by this phase. We believe that this material corresponds to a quenched liquid, which is denoted as glass in Table 2, produced by the partial melting of the bulk sample. Although we could not analyze precisely the composition of this amorphous phase, EDS analyses show that it is composed of Ti, B, and O, and the proportion of these elements changes with the temperature.

The compositions #2 and #3 correspond to H_3BO_3 + TiO_2 (1:1), and HBO_2 + TiO_2 (1:1), respectively. Experiments in both compositions were made at temperatures higher than 600 °C, and the results are similar as shown in Table 2. The Raman spectra in Figure 3 showed peaks characteristic of TiO_2-II at low temperatures, that were replaced by peaks of rutile at 800 °C for both compositions. At low temperatures, HBO_2-II is the stable phase; however, it disappears at temperatures around 850 °C, for composition #2, and around 900 °C, for composition #3.

The composition #4 corresponds to B_2O_3 + TiO_2 (1:1), in which 10 mol % of water was added with a microsyringe. This composition is assumed to be lower than that necessary to transform all B_2O_3 in H_3BO_3. Because of the previous heating at 1000 °C, all TiO_2 is present as rutile in the starting material. The Raman spectra of the samples processed at temperatures from 800 to 1000 °C are displayed in Figure 4, showing rutile phases a very sharp peak at 783 cm^{-1}, with a shoulder at 770 cm^{-1}, which is characteristic of HBO_2-II. At temperatures higher than 1000 °C, the characteristic peaks of HBO_2-II decrease, and a peak at 725 cm^{-1} appears. We believe that this indicates the onset of B_2O_3 crystallization.[24]

In all experiments with compositions #1, #2, #3, and #4, the amorphous material interpreted as glass was present. Rutile is always the stable phase above 800 °C; however, it differs from the starting material by the shift of the peak from 612 to 607 cm^{-1}. These results are in agreement with Mammone et al.[19] that suggested an irreversible transformation of anatase and rutile to TiO_2-II around 7.0 ± 0.5 GPa. Moreover, our experiments indicate that TiO_2-II transforms to rutile at high-pressure (7.7 GPa) above 800 °C.

Discussion

In the P−T range considered in this work, B_2O_3 is probably far below its critical point, and this conclusion comes from its observed boiling point at 1 atm, around 2400 °C.[25] This observation and the data from this work enable the summarization of the experimental results in Table 2. The phases recognized as primary phases are rutile, anatase, and TiO_2-II, as TiO_2 phases; boric acid (sassolite) and orthorhombic metaboric acid, representing the hydrous boric oxide phases; B_2O_3 crystal, representing the anhydrous boric oxide phase; and the glass phase, representing the quenched liquid phase (L).

(24) Bronswijk, J. P.; Strijks, E. *J. Non-Cryst. Solid* **1977**, *24*, 145.
(25) Soulen, J. R.; Margrave, J. L. *J. Am. Chem. Soc.* **1956**, *78*, 2911.

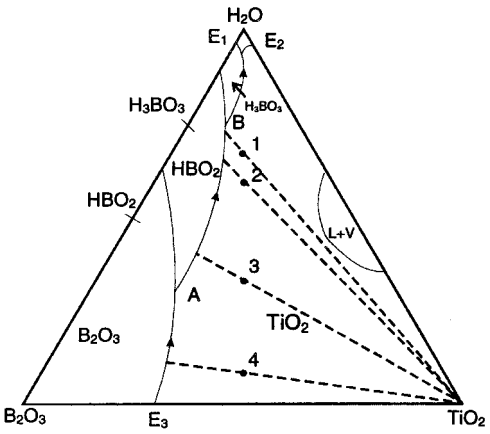

Figure 5. Schematic phase diagram for the system TiO_2–B_2O_3–H_2O at 7.7 GPa. Dots: bulk compositions (Table 1) investigated in this study. L+V field determines the L ↔ V reaction. A represents the piercing point of the reaction $B_2O_3 + TiO_2 + L_1 \leftrightarrow HBO_2 + TiO_2 + L_2$ at around 1100 °C, and B represents the piercing point of the reaction $HBO_2 + TiO_2 + L_3 \leftrightarrow H_3BO_3 + TiO_2 + L_4$ at around 600 °C. Compositions of L_1, L_2, L_3, and L_4 were not determined. The direction of decreasing *T* is given by the arrows in the cotectic lines (solid lines). Dashed lines correspond to tie lines. E_1, E_2, and E_3 represent the eutectic points.

These results suggest the following reactions and piercing points:

$$B_2O_3 + TiO_2 + L_1 \leftrightarrow HBO_2 + TiO_2 + L_2 \text{ at around 1100 °C} \quad (1)$$

$$HBO_2 + TiO_2 + L_3 \leftrightarrow H_3BO_3 + TiO_2 + L_4 \text{ at around 600 °C,} \quad (2)$$

where L_1, L_2, L_3, and L_4 are liquid with different Ti/B ratios. TiO_2 can occur as anatase and rutile, at low temperature, as TiO_2-II up to 800 °C, and as rutile above 800 °C. Its behavior is not represented in the reactions depicted above.

Following these assumptions, a polythermal, isobaric diagram is suggested in Figure 5. However, the position of the cotectic lines and piercing points in the diagram are only schematic due to lack of analysis of the melt composition (glass phase). The elaboration of this schematic ternary phase diagram obeyed the following premises:

(a) All cotectic lines must be on the left side of the line that connects all the compositions of the starting materials (denoted by the numbers 1, 2, 3, and 4), due to the characteristics of the system as, for example, the solubility and the melting point of the phases.

(b) The cotectic piercing point (A) defined by the reaction 1 must be placed between the projection of the tie line of the composition 4 and 3, on the cotectic lines, according to the experimental results.

(c) The cotectic piercing point (B) defined by the reaction 2 must be placed beyond the projection of the tie line of the composition 1 on the cotectic lines.

At pressures of 5 and 10 GPa, H_2O melts at 230 and 315 °C, respectively,[26] and all compositions used to build this diagram are out of the solid H_2O stability field. This feature suggests that the vapor field and the vapor–liquid boundary are reduced in the conditions of these experiments, and that B_2O_3 together with H_2O are soluble in the liquid. EDS analyses in the quenched liquid emphasize this assumption. Optical microscope observation and electron microscopic images do not suggest liquid–liquid immiscibility in any composition studied to build this diagram at 7.7 GPa.

Vitreous B_2O_3 (v-B_2O_3) consists of boroxol groups (B_3O_6), which is a three-membered ring of BO_3 triangles, constrained to be planar by delocalized π bonding.[27] The breathing mode of this boroxol group is Raman active and characterized by a sharp peak at 808 cm^{-1}. High-pressure monitoring of this peak has shown that with increasing pressure, the peak shifts up to 810 cm^{-1}, up to 16 GPa, when it disappears. With the pressure release, this peak reappears, but with lower intensity.[28] With addition of alkalis (M_2O, M = K or Na) up to R = 0.5 (R = [mol % M_2O]/[mol % B_2O_3]), the boroxol groups are progressively replaced by structural units with tetrahedral coordination of B atoms[29,30] (tetraborate, six-membered borate rings with one and maybe two BO_4 tetrahedrons, diborate groups). To obtain some information about the glass phase produced in this study, all compositions were processed to temperatures higher than the cotectic temperatures. This procedure increases the amount of glass in the capsule. Raman analysis of the glass phase was performed on all samples, and no peaks were observed. From these data, it is not possible to ascertain that B is arranged in boroxol groups. The EDS analysis shows only that Ti, B, and O are present in this liquid. Microscopic investigation does not show immiscibility of phases. This information suggests that any liquid composed of oxygen-bearing phases, present during sintering of TiB_2 at high-pressure,[31] could be the medium for material transporting, contributing to the grain growth and decrease of hardness and density of ceramics composed of TiB_2.

Conclusions

The system TiO_2–H_2O–B_2O_3 was studied at high-pressure (7.7 GPa) and high temperatures, and a phase diagram was schematically proposed. The eutectic point was identified to be at around 400 °C. Two piercing points where identified at around 600 and 1100 °C, with the stabilization of HBO_2 rather than H_3BO_3, and the stabilization of B_2O_3 rather than HBO_2, respectively. Besides its fundamental scientific interest, this study can be directly applied to help understanding of the sintering of borides such as TiB_2, in which the presence of oxygen-bearing phases decreases the eutectic point of the system. This phenomenon can produce a melt phase that could act as a medium for material transport and produce grain growth influencing the sintering and tribological properties of the ceramic.

Acknowledgment. The authors thank FAPERGS, FINEP, PADCT III/CNPq, PRONEX/MCT for the financial support.

CM0103242

(26) Pistorius, C. W.; Rapoport, E.; Clark, J. B. *J. Chem. Phys.* **1968**, *48*, 5509.
(27) Johnson, P. A. V.; Wright, A. C.; Sinclair, R. N. *J. Non-Cryst. Solids* **1982**, *50*, 281.
(28) Grimisditch, M.; Polian, A.; Wright, A. *Phys. Rev. B.* **1996**, *54*, 152.
(29) Konijnendjik, W. L.; Stevels, J. *M. Verres Refract.* **1976**, *30*, 821.
(30) Yun, Y. H.; Bray, P. J. *J. Non-Cryst. Solids* **1978**, *27*, 363.
(31) Soares, S. R. S., unpublished results.